

# 1 **Supplementary material**

2 Table of Contents

3 **Supplementary Material A:** Steps to idealise an ellipse from a landslide  
4 polygon.

5 **Supplementary Material B:** Kolmogorov-Smirnov testing of distribution of  
6 landslide ellipse length-to-width ratio ( $\Lambda_E$ ) between landslide area categories.

7 **Supplementary Material C:** Modified Kolmogorov-Smirnov goodness-of-fit test  
8 for probability density functions fit to landslide ellipse length-to-width ratio within  
9 each landslide area category.

10 **Supplementary Material D:** Python Grass-GIS code for fitting an ellipse to  
11 landslide polygon.

12 **Supplementary Material E:** R Code for inverse-Gamma probability density  
13 function fitting of length-to-width ratio.

14

15

16

## Supplementary Material A

17

### Steps to idealise an ellipse from a landslide polygon

18

19 Here we outline the six steps for calculating the length-to-width ratio of an idealised ellipse  
20 from a landslide polygon. These provide further detail and justification to supplement **Tables**  
21 **III and IV** (main text).

22 *Step A: Preliminary landslide spatial attributes.* For elliptic approximation Methods 1 to 3  
23 (**Table III**, main text), we first use existing GIS tools to calculate the centre of gravity and  
24 orientation of the original landslide shape, which has a landslide area ( $A_L$ ) and perimeter ( $P_L$ ).  
25 The centre of gravity is based on a weighted mean of the landslide shape's Northing and  
26 Easting coordinates (N, E) (Khorshidi, 2009) and forms the map coordinates that define the  
27 centre point of the final best-fit elliptic shape. In a small number of cases, it is possible for the  
28 centre of gravity to fall outside of the original landslide shape's extent. The orientation of the  
29 original landslide is calculated in a GIS, which is used to align the landslide best-fit ellipse's  
30 long axis.

31 *Step B: Fit convex hull.* For the elliptic approximation Method 2 and Method 3, a convex hull  
32 (CH) is fit to the original landslide shape using dedicated tools within a GIS. A convex hull is  
33 the smallest shape that completely contains the perimeter of the original landslide shape,  
34 where all internal angles of the CH are less than  $180^\circ$  (de Berg *et al.*, 2008). The area ( $A_{CH}$ )  
35 and perimeter ( $P_{CH}$ ) of the CH are then used as the inputs to the following Step C. Within the  
36 GIS,  $A_{CH}$  is calculated using the shoelace algorithm (ESRI, 2016) and  $P_{CH}$  using Pythagorean  
37 theorem (Prashker, 1999).

38 *Step C: Calculate ellipse length-to-width ratio from area and perimeter of the original landslide*  
39 *shape or the CH fit.* In order to 'simplify' the asymmetric and irregular shape of landslide  
40 polygons to a regular ellipse, we can use the area and perimeter of the original landslide  
41 shape ( $A_L$ ,  $P_L$ ) or the CH fit to the landslide shape ( $A_{CH}$ ,  $P_{CH}$ ), to estimate the ellipse length-  
42 to-width ratio ( $\Lambda_E = L_E/W_E$ ) with the same area and perimeter as the original or CH shape.

43 The length-to-width ratio  $\Lambda_E$  for an idealised elliptic shape is calculated using the solution to  
44 a quadratic equation, based on the equations for ellipse area and perimeter. The area of an  
45 ellipse  $A_E$ , is calculated as (Heath, 1931),

$$A_E = \pi ab \quad \text{Eq. (S1)}$$

46 where  $a$  = semi-major axis of ellipse,  $b$  = semi-minor axis of ellipse. Calculating the exact  
 47 perimeter of an ellipse ( $P_E$ ) is complex, so it is common to use a variety of elliptic  
 48 approximations based on the long ( $a$ ) and short ( $b$ ) axes of the ellipse. Here, due to its relative  
 49 simplicity, we use Euler's (1773) formula (described in Michon, 2015),

$$P_E \approx \pi\sqrt{2(a^2 + b^2)} \quad \text{Eq. (S2)}$$

50 where  $P_E$  = ellipse perimeter,  $a$  = semi-major axis of ellipse,  $b$  = semi-minor axis of ellipse.  
 51 We note that this approximation for  $P_E$  can be up to 10% inaccurate for very long, thin ellipses  
 52 (Michon, 2015). By combining **Eqs. S1** and **S2**, we can solve for the length-to-width ratio of  
 53 an ellipse ( $a/b$ ) = ( $L_E/W_E$ ), in terms of the area ( $A_E$ ) and perimeter ( $P_E$ ) of the ellipse, by using  
 54 the solution to a quadratic equation, giving,

$$\lambda_E = \frac{L_E}{W_E} = \frac{4\pi A_E}{P_E^2 - \sqrt{P_E^4 - 16\pi^2 A_E^2}} \quad \text{Eq. (S3)}$$

55 We then substitute into **Eq. S3** the area ( $A_E$ ) and perimeter ( $P_E$ ) of the ellipse with the area  
 56 and perimeter of original landslide shape ( $A_L$ ,  $P_L$ ), or the CH fit to the landslide shape ( $A_{CH}$ ,  
 57  $P_{CH}$ ), thus approximating the length-to-width ratio ( $\lambda_E$ ) of an idealised elliptic shape with the  
 58 same area and perimeter as that of the original landslide or the CH fit.

59 When substituting the original landslide  $P_L$  for the ellipse  $P_E$ , **Eq. S3** becomes sensitive to the  
 60 original landslide's perimeter 'sinuosity' relative to its area ( $A_L$ ). If the original landslide has a  
 61 'sinuous' perimeter ( $P_L$ ), this has the potential to force the idealised elliptic shape to longer,  
 62 thinner forms. For this reason, we fit a CH to the original landslide shape which removes most  
 63 internal voids from the landslide shape.

64 *Step D: Calculate ellipse length and width from length-to-width-ratio and area.* The ellipse  
 65 length ( $L_E$ ) and width ( $W_E$ ) can then be expressed in terms of the length-to-width ratio of the  
 66 ellipse  $\lambda_E$  and the landslide area ( $A_L$ ) or area of the CH fit ( $A_{CH}$ ) which we denote as  $A$ :

$$\begin{aligned} L_E &= 2\sqrt{\frac{A\lambda_E}{\pi}} \\ W_E &= 2\sqrt{\frac{A}{\pi\lambda_E}} \end{aligned} \quad \text{Eq. (S4)}$$

67 *Step E: Scale ellipse area to match original landslide area.* For elliptic approximation Method  
68 3 the length ( $L_E$ ) and width ( $W_E$ ) of the ellipse approximated from a CH fit to the original  
69 landslide shape is scaled so that the area of the CH ( $A_{CH}$ ) matches the area of the original  
70 landslide,

$$L_{Scaled\ CH} = L_{CH} \sqrt{\frac{A_L}{A_{CH}}}$$
$$W_{Scaled\ CH} = W_{CH} \sqrt{\frac{A_L}{A_{CH}}}$$

Eq. (S5)

71 This scaling does not affect the 'shape' of the ellipse in terms of  $\Lambda_E$ , but can result in a better  
72 match in terms of area between the idealised elliptic shape ( $A_E$ ) and the original landslide  
73 shape.

74 *Step F: Plot ellipse from length, width, centroid and orientation.* The final stage of elliptic  
75 approximation Methods 1 to 3 is to plot the ellipse using standard GIS tools. The inputs to  
76 the GIS tools are (i) ellipse length ( $L_E$ ) and width ( $W_E$ ); (ii) ellipse centroid coordinates, which  
77 correspond with where the length and width segments intersect; and (iii) ellipse orientation,  
78 which corresponds to the angle of orientation of the ellipse long axis  $L_E$ . The output is an  
79 elliptical approximation of the original landslide shape, which should approximately align with  
80 and overlay the original landslide.

81

82

## Supplementary Material B:

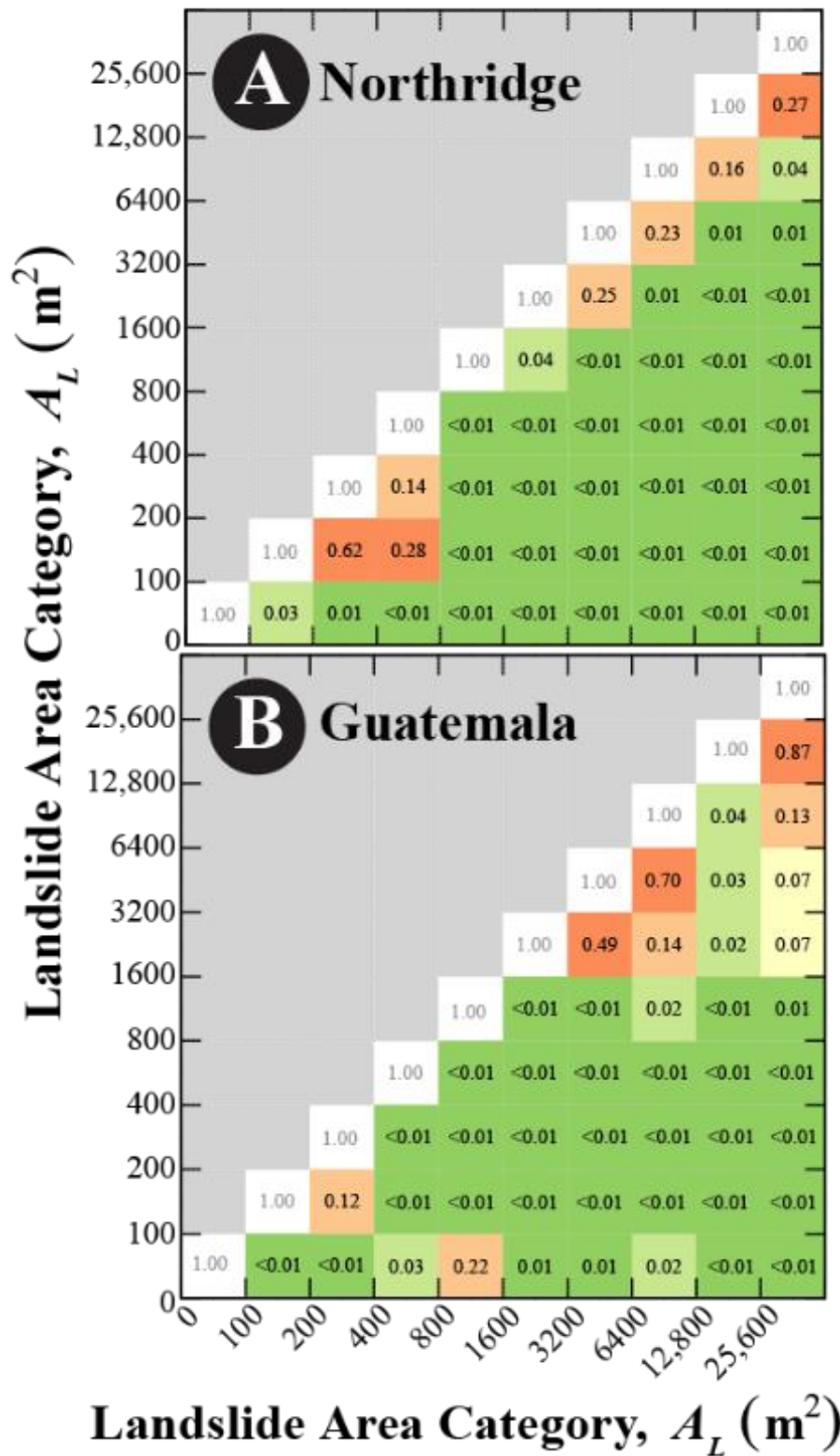
### Kolmogorov-Smirnov testing of distribution of landslide ellipse length-to-width ratio ( $\Lambda_E$ ) between landslide area categories.

In this supplementary material we describe the use of a Kolmogorov–Smirnov (K–S) two-sample test (Liliefors, 1967) to compare the distribution of  $\Lambda_E$  for each of the two landslide inventories in the ten landslide area categories, numbered 1 to 10 with 1 being the smallest landslide area category and 10 the largest (Figure S1, left to right along the x-axis), using the following hypothesis:

$H_0$  The  $\Lambda_E$  values in landslide area category  $i$  come from the same statistical one-point probability distribution as the  $\Lambda_E$  values in landslide area category  $j$ , where  $i$  and  $j$  represent the ten different categories of landslide areas given in Figure S1,  $i \neq j$ ,  $i = 1, 2, \dots, 10$ ;  $j = 1, 2, \dots, 10$ .

$H_1$  The  $\Lambda_E$  values in landslide area category  $i$  do not come from the same statistical one-point probability distribution as the  $\Lambda_E$  values in landslide area category  $j$ , where  $i$  and  $j$  represent the ten different categories of landslide areas given in Figure S1,  $i \neq j$ ,  $i = 1, 2, \dots, 10$ ;  $j = 1, 2, \dots, 10$ .

In its standard form, the two-sample K–S test measures the maximum distance ( $D$ ) between two empirical cumulative frequency curves (Liliefors, 1967). Here, we will compare the cumulative frequencies of  $\Lambda_E$  for each pair of  $A_L$  categories. If the maximum distance ( $D$ ) between the two empirical curves (each based on a different landslide area category) is small, this suggests both datasets ( $F_i(x)$  and  $F_j(x)$ ) follow approximately the same statistical one-point probability distribution. If  $D$  is large, this suggests significant deviation between the two cumulative distribution functions (Wilcox, 2005). The maximum distance  $D$  is then compared to already established tables to calculate the probability,  $p$ , that this magnitude of  $D$  would have been observed if the two datasets did truly come from the same distribution. Figure S1 shows the K–S test  $p$  value results of comparing each landslide area category ( $A_L$ ) to each other for Northridge and then Guatemala.



112

113 **Figure S1.** Probability  $p$  values from the two-sample Kolmogorov–Smirnov tests to compare  
 114 distributions of landslide length-to-width ratio ( $\lambda_E$ ) between each landslide area category. **(A)**  
 115 9,441 landslides in the 1994 Northridge landslide inventory and **(B)** 8,031 landslides in the  
 116 1998 Guatemala landslide inventory. Box colours correspond to the significance of the  $p$ -  
 117 value, where green denotes very low  $p$ -values (i.e., there is a low probability the samples  
 118 were drawn from the same distribution) and orange denotes high  $p$ -values (i.e., there is a  
 119 high probability the samples were drawn from the same distribution). Values of  $p = 0.00$   
 120 denote very small values of  $p$  (e.g.,  $p < 10^{-3}$ ) rounded to 0.00.

121 Using a significance level of  $p = 0.10$ , results in 38 out of 45 pairs of  $A_L$  categories where the

122 null hypothesis is rejected that the probability density distribution of  $\Lambda_E$  is the same in both  $A_L$   
123 categories. The  $p$  values are generally higher in neighbouring landslide area categories for  
124 the 'tails' of the categories (i.e., very small and very large landslide areas), which is attributed  
125 to small sample sizes in these categories. Broadly there is a difference in the distribution of  
126  $\Lambda_E$  between pairs of landslide area categories, with some discrepancies.

127

128

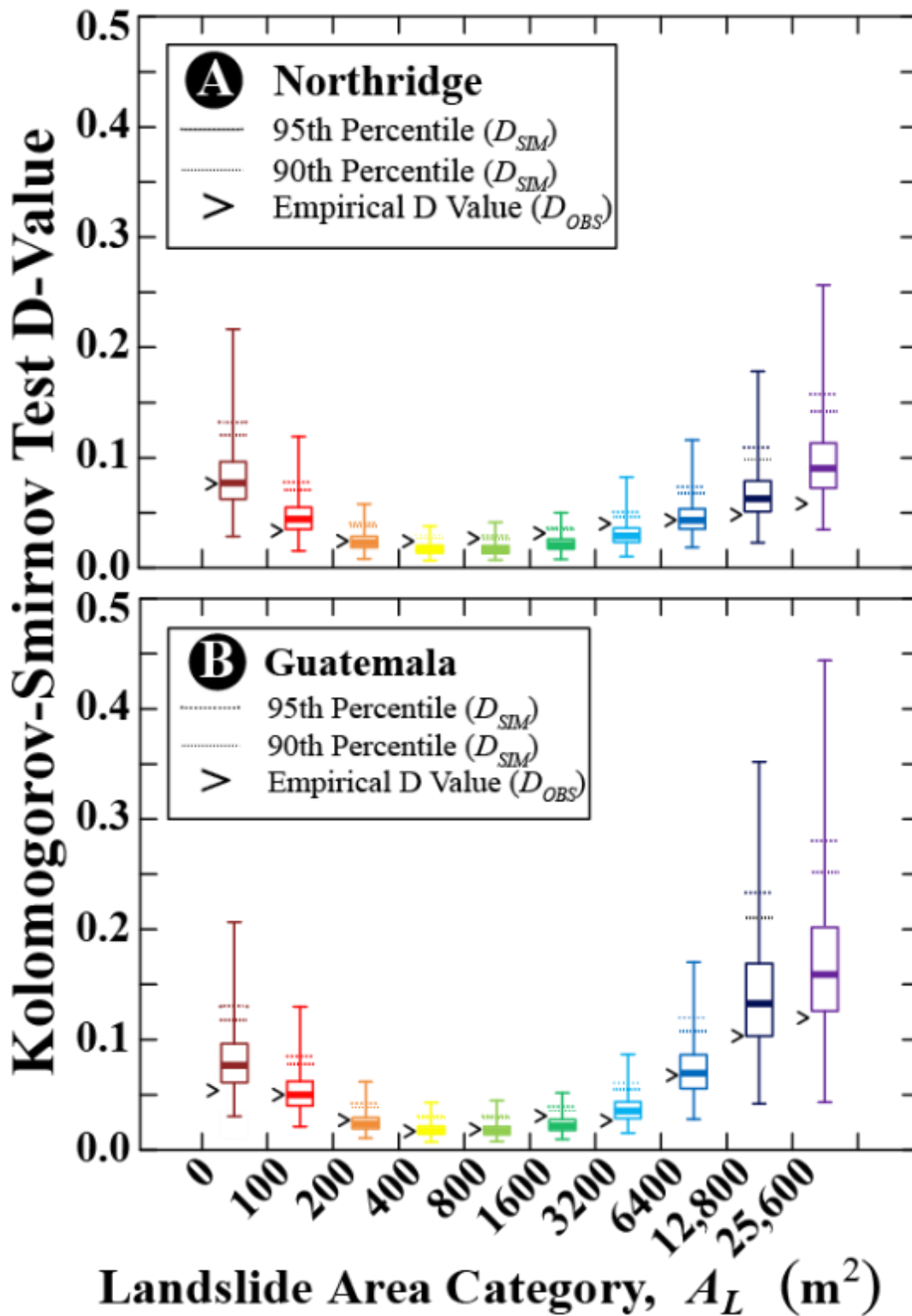




163 (here, we chose 2,500 iterations). In each case, the values  $\rho_{\text{SIM}}$ ,  $a_{\text{SIM}}$ ,  $s_{\text{SIM}}$  will vary slightly.  
164 For each iteration, record  $D_{\text{SIM}}$ .  
165 7. Compare  $D_{\text{OBS}}$  to the range of  $D_{\text{SIM}}$ . The significance level ( $p$ ) is defined by the percentile  
166 of  $D_{\text{SIM}}$ , i.e., to test the data to  $p = 0.90$  significance level, compare  $D_{\text{OBS}}$  to the 90<sup>th</sup>  
167 percentile of  $D_{\text{SIM}}$ . If  $D_{\text{OBS}} < (p \times D_{\text{SIM}})$ , we can accept the null hypothesis that the observed  
168  $\Lambda_E$  data come from the inverse-Gamma pdf with parameters  $\rho_{\text{OBS}}$ ,  $a_{\text{OBS}}$ ,  $s_{\text{OBS}}$ .

169 This method works on the premise that the observed (empirical) data can be considered to  
170 have come from the same distribution as that fit to it if the  $D$  value lies within the normal range  
171 of those encountered when fitting a distribution to random deviates from a known distribution.  
172 **Figure S2** shows boxplots of the distribution of  $D_{\text{SIM}}$  values and  $D_{\text{OBS}}$  for each landslide area  
173 category for both Northridge and Guatemala.

174



175

176 **Figure S2.** Boxplots of  $D_{SIM}$  values from Monte-Carlo Kolmogorov–Smirnov goodness-of-fit  
 177 testing, compared to the observed  $D_{OBS}$  value (indicated by >). The upper and lower  
 178 horizontal lines of the boxplot rectangles represent the interquartile range of the  $D_{SIM}$  values  
 179 (25<sup>th</sup> and 75<sup>th</sup> percentiles), the thick horizontal lines the median  $D_{SIM}$  (50<sup>th</sup> percentile), the  
 180 boxplot upper and lower horizontal lines the maximum and minimum  $D_{SIM}$  values. Also shown  
 181 for each boxplot are the 95<sup>th</sup> percentile for the  $D_{SIM}$  values and represented by dotted  
 182 horizontal lines and the 90<sup>th</sup> percentile by dashed horizontal lines.

183

184 For all landslide area categories for both the Northridge and Guatemala landslide inventories

185 in **Figure S2**,  $D_{OBS}$  (indicated by the symbol  $>$  next to each boxplot) is below the 95<sup>th</sup> and 90<sup>th</sup>  
186 percentile of  $D_{SIM}$  values (indicated by the dotted and dashed horizontal dashed lines,  
187 respectively) and corresponding to  $p = 0.05$  and  $p = 0.10$ , respectively. This suggests that  
188 the deviations between observations and the best-fit pdf are within the ‘normal range’ to be  
189 expected if the data were drawn from that distribution. We therefore conclude from **Figure**  
190 **S2** that the 20 inverse-Gamma pdfs shown in **Figure 10** (main text) are reasonable models  
191 for the distribution of landslide ellipse  $\Lambda_E$  for both Northridge and Guatemala.

192

193 **Supplementary Material D**

194 **Python Grass-GIS code for fitting an ellipse to landslide polygon**

195

196 This Python code utilises Grass-GIS tools to fit an ellipse to each landslide polygon in an  
197 inventory. It then measures the goodness-of-fit of each ellipse using the ellipticity index ( $e_L$ )  
198 (Eq. 4, main text) and the length-to-width ratio of the ellipse ( $\Lambda_E$ ) (Eqs. 1-3, main text). The  
199 workflow is shown in Figure 4 (main text)

200 Available to download from:

201 [https://github.com/faithatron/Landslide\\_shape\\_tools/](https://github.com/faithatron/Landslide_shape_tools/)

202

203 **Supplementary Material E**

204 **R Code for Inverse Gamma probability density function fitting of length-**  
205 **to-width ratio**

206

207 This R code will perform maximum likelihood estimation fitting of an inverse-Gamma  
208 probability density function (pdf) (**Eq. 5**) to landslide length-to-width ratios ( $\Lambda_E$ ) generated  
209 using the Grass-GIS model code in **Supplementary Material D**. A bootstrapping technique  
210 (**Supplementary Material C**) is used to test the goodness-of-fit of the model pdf to the  
211 original data and add error bars to the plots of the pdf. The R code will generate a figure  
212 similar to **Figure 10** (main text) showing the best fit pdf to the observed data for each landslide  
213 area category. Comments are included in the code to explain the steps.

214 Available to download from:

215 [https://github.com/faithatron/Landslide\\_shape\\_tools/](https://github.com/faithatron/Landslide_shape_tools/)

216

217